J|A|C|S
ARTICLES

Published on Web 05/13/2010

Charge-Mediated Adsorption Behavior of CO on MgO-Supported Au Clusters

Xiao Lin,[†] Bing Yang,[†,‡] Hadj-Mohamed Benia,[†] Philipp Myrach,[†] Maxim Yulikov,[†] Andreas Aumer,[†] Matthew A. Brown,[†] Martin Sterrer,[†] Oleksander Bondarchuk,[†] Esther Kieseritzky,[†] Jan Rocker,[†] Thomas Risse,[†] Hong-Jun Gao,[‡] Niklas Nilius,*[,†] and Hans-Joachim Freund[†]

Fritz-Haber-Institut der MPG, Faradayweg 4-6, D-14195 Berlin, Germany and Institute of Physics, Chinese Academy of Sciences, P.O. Box 603, Beijing 100190, China

Received February 17, 2010; E-mail: nilius@fhi-berlin.mpg.de

Abstract: The CO binding behavior to gold particles supported on MgO thin films has been analyzed with scanning tunneling microscopy (STM) and infrared spectroscopy (IRAS). The ad-particles accommodate excess electrons that originate either from a charge transfer through the thin oxide film or from a local interaction with electron-rich oxide defects that act as Au nucleation centers. The enhanced electron density in the Au aggregates affects both the spatial distribution and the vibrational properties of adsorbed CO species. Whereas preferential CO attachment to the chemically unsaturated and electron-rich boundary sites of the Au islands is deduced from the STM data, a continuous downshift of the CO stretching frequency with decreasing particle size is observed in IRAS. Both results are interpreted in the light of CO adsorption to negatively charged metal aggregates and used to draw general conclusions on the interplay between charge and adsorption properties of confined metal systems.

Introduction

The binding of molecules to specific sites of a metal nanoparticle is thought to determine the reactivity of metal/oxide systems used in heterogeneous catalysis.[1] Recent studies have suggested that the particle charge state has an influence on the chemical properties as well.[2,3] In particular, excess electrons are expected to facilitate the bond cleavage of molecular adsorbates, e.g. of O_2, thereby improving the catalytic performance of the system.[4] Direct experimental insight into molecular binding schemes to metal particles is however scarce, and little is known on the interplay between the morphologic and electronic structure of a particle and its adsorption properties.

The present knowledge on the adsorption behavior of oxide-supported metal particles mainly derives from nonlocal experimental approaches, such as infrared-reflection-absorption spectroscopy (IRAS).[5−8] The interpretation of such experiments often relies on analogies to simple model systems and theoretical studies.[9,10] In contrast, spatially resolving techniques such as scanning tunneling microscopy (STM) are capable of providing direct insight into the binding environment of adsorbates. The application of STM is however restricted to sufficiently conductive and weakly corrugated surfaces that may nonetheless mimic the properties of supported metal catalysts.[7,8,11]

In this paper, we combine STM and IRAS to investigate CO adsorption on Au particles anchored to MgO(001) thin films. This system has recently attracted a lot of interest, as the charge on the ad-particles is an adjustable quantity.[8,12,13] This flexibility renders charge-dependent adsorption studies feasible not only in the gas phase[14] but on a solid surface. Two mechanisms are responsible for the electron exchange between the MgO film and the metal ad-particles. On ultrathin films grown on Ag(001) and Mo(001), charge transfer is initiated by different chemical potentials of the Au deposits and the metal/oxide support, being

[†] Fritz-Haber-Institut der MPG.
[‡] Chinese Academy of Sciences.

(1) Ertl, G.; Knözinger, H.; Weitkamp, J., Eds. *Handbook of Heterogeneous Catalysis*; Wiley: Weinheim, 1997.
(2) Fu, Q.; Saltsburg, H.; Flytzani-Stephanopoulos, M. *Science* **2003**, *301*, 935.
(3) Sauer, J.; Döbler, J. *Dalton Trans.* **2004**, *19*, 3116–3121. Zhai, H.-J.; Döbler, J.; Sauer, J.; Wang, L.-S. *J. Am. Chem. Soc.* **2007**, *129*, 13270–13276.
(4) Molina, L. M.; Hammer, B. *Appl. Catal., A* **2005**, *291*, 21–31.
(5) Zecchina, A.; Scarano, D.; Bordiga, S.; Ricchiardi, G.; Spoto, G.; Geobaldo, F. *Catal. Today* **1996**, *27*, 403–435.
(6) Street, S. C.; Xu, C.; Goodman, D. W. *Annu. Rev. Phys. Chem.* **1997**, *48*, 43–68.
(7) Meyer, R.; Lemire, C.; Shaikhutdinov, S.; Freund, H.-J. *Gold Bull.* **2004**, *37*, 72–124. Lemire, C.; Meyer, R.; Shaikhutdinov, S.; Freund, H.-J. *Angew. Chem., Int. Ed.* **2004**, *43*, 118–121.
(8) Sterrer, M.; Yulikov, M.; Fischbach, E.; Heyde, M.; Rust, H.-P.; Pacchioni, G.; Risse, T.; Freund, H.-J. *Angew. Chem., Int. Ed.* **2006**, *45*, 2630–2632.
(9) Sicolo, S.; Giordano, L.; Pacchioni, G. *J. Phys. Chem. C* **2009**, *113*, 10256–10263.
(10) Giordano, L.; Martinez, U.; Sicolo, S.; Pacchioni, G. *J. Chem. Phys.* **2007**, *127*, 144713.
(11) Nilius, N. *Surf. Sci. Rep.* **2009**, *64*, 595–659.
(12) Sterrer, M.; Yulikov, M.; Risse, T.; Freund, H.-J.; Carrasco, J.; Illas, F.; Di Valentin, C.; Giordano, L.; Pacchioni, G. *Angew. Chem., Int. Ed.* **2006**, *45*, 2633–2635.
(13) Lin, X.; Nilius, N.; Freund, H.-J.; Walter, M.; Frondelius, P.; Honkala, K.; Häkkinen, H. *Phys. Rev. Lett.* **2009**, *102*, 206801. Lin, X.; Nilius, N.; Sterrer, M.; Koskinen, P.; Häkkinen, H.; Freund, H.-J. *Phys. Rev. B*, **2010**, *81*, 153406.
(14) Fielicke, A.; von Helden, G.; Meijer, G.; Simard, B.; Rayner, D. M. *J. Phys. Chem. B* **2005**, *109*, 23935–23940.

compensated by an electron flow toward the gold.[15] On thicker films, charge might be transferred from electron traps in the oxide surface, e.g. oxygen vacancies and dislocation lines, into the ad-particles.[16] In both cases, CO can be used as a probe molecule, as its adsorption is known to be sensitive to structural and electronic peculiarities of the local environment. The observed binding behavior is hereby interpreted with the help of two established concepts. The first one is the bond-order-conservation model that accounts for the increasing tendency of low-coordinated surface sites to bind molecules from the gas phase. The second one is the Blyholder model,[17] which explains CO bonding to metals in terms of σ-donation from the CO lone pair into accepting metal states and π-back-donation of metal electrons into the empty CO $2\pi^*$ orbital. Especially, the latter contribution is conveniently probed with IRAS, as it induces a downshift of the CO stretching frequency. The experimental results presented here provide insight into the interrelation between the topology and charge state of Au particles and their adsorption behavior.

Experiment

Two adsorption systems have been used in this study, a 2−3 ML MgO film on Ag(001)[18] and a 12−15 ML MgO film grown on a Mo(001) support.[19] A monolayer is hereby defined as one oxide Mg^{2+} ion per metal atom in the support or correspondingly as 1.13×10^{15} Mg^{2+} per cm^2. Both films are prepared by Mg deposition in 1×10^{-6} mbar O_2 at 550 K. The MgO/Mo film is annealed to 1100 K after deposition to improve its crystallinity. Whereas thin MgO/Ag films are generally defect poor due to the good match of both lattice constants (3%),[18] a high density of dislocation lines is observed in the Mo-supported MgO films (5.4% mismatch).[19] F^0 and F^+ color centers are introduced into thicker films by bombarding them with 100 eV electrons.[8] The abundance of such electron-rich defects facilitates charge transfer processes into ad-particles. Gold (0.005−0.1 ML) is deposited from a Mo crucible onto the MgO/Ag and the MgO/Mo films at 150 and 30 K, respectively. On the Ag-supported films, gold forms planar islands with (111) termination.[13] This particular growth mode reflects the high interfacial adhesion that originates from the charge transfer between the MgO/Ag support and the Au deposits.[20] On thicker MgO/Mo films, misfit dislocations are the preferred nucleation sites, while few terrace-bound particles form due to Au attachment to the artificially introduced point defects.[21] In contrast to the MgO/Ag system, the Au particles adopt more prolate shapes, although they are expected to be negatively charged as well. In a final preparation step, both systems are saturated with CO at 30 K.

Results and Discussion

CO Adsorption on Au Islands on Thin MgO/Ag Films. Single CO molecules are identified as 0.25 Å deep, circular depressions in the oxide film (Figure 1a).[22] A similar imaging contrast is observed on most metal surfaces, where it originates from the absence of CO orbitals for tunneling transport close to the Fermi level (E_F). CO attachment to the tip gives rise to a distinct contrast change of the adsorbates, which now appear as dark rings of ~8 Å diameter (Figure 1b). This new imaging mode results from interference effects between various adsorbate-mediated conductance channels.[23] It enables CO identification even on corrugated surfaces, e.g. next to a Au deposit, where the tiny CO-induced depressions obtained with metallic tips are no longer detectable. Figure 1c shows a corresponding STM image of a Au island saturated with CO. Apparently, the CO-induced features are exclusively localized along the island perimeter, while the center remains adsorbate-free. CO attachment to the island boundary has been observed for several other Au clusters in this study.

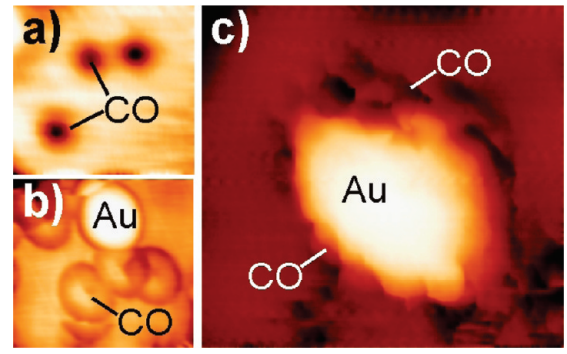

Figure 1. STM topographic images of CO molecules on 2 ML MgO/Ag(001) imaged with (a) a metallic and (b) a CO-covered tip (3×3 nm^2, 150 mV, 3pA). The CO(tip)−CO(sample) interaction leads to a ring-like appearance of the adsorbates in (b). (c) STM image of a CO-saturated Au island taken with a CO-covered tip (4×4 nm^2, 100 mV, 3pA). CO-induced contrast is only revealed at the perimeter of the Au island.

An alternative method to identify CO molecules on the oxide surface would be inelastic-electron-tunneling spectroscopy (IETS) with the STM.[24,25] This technique probes the availability of inelastic transport channels between tip and sample that open due to an energy transfer from the tunneling electrons to molecular degrees of freedom. The resulting increase of the conductance gives rise to a step in the first bias derivative of the tunnel current (dI/dV) and to a peak/dip structure in the second-derivative signal (d^2I/dV^2). The peak/dip position hereby corresponds to the positive/negative vibrational energy of the mode, respectively. The CO vibrational mode with the highest excitation cross section in STM-IETS is the frustrated rotation.[24] It has been detected at ~45 ± 5 meV for Au monocarbonyls on MgO/Ag(001), which compares to a calculated value of 39 meV.[22] Consequently, bias voltages of ±45 mV have been chosen here to identify CO molecules next to the 2D Au islands via their vibrational signature (Figure 2). As before, no CO is visible on the aggregate in topographic images taken with a metallic tip. However, CO related loss signals emerge in the d^2I/dV^2 maps and produce a bright/dark brim around the island at positive/negative sample bias (Figure 2c,d). Control measurements taken at bias values above or below the CO frustrated rotation did not produce any d^2I/dV^2 contrast (Figure 2b). The localization of the inelastic signals along the perimeter therefore

(15) Pacchioni, G.; Giordano, L.; Baistrocchi, M. *Phys. Rev. Lett.* **2005**, *94*, 226104.
(16) Del Vitto, A.; Pacchioni, G.; Delbecq, F. O.; Sautet, P. *J. Phys. Chem. B* **2005**, *109*, 8040–8048.
(17) Blyholder, G. *J. Phys. Chem.* **1964**, *68*, 2772–2778.
(18) Schintke, S.; Messerli, S.; Pivetta, M.; Patthey, F.; Libjoulle, L.; Stengel, M.; de Vita, A.; Schneider, W. D. *Phys. Rev. Lett.* **2001**, *87*, 276801.
(19) Benedetti, S.; Benia, H. M.; Nilius, N.; Valeri, S.; Freund, H.-J. *Chem. Phys. Lett.* **2006**, *430*, 330–335. Benedetti, S.; Torelli, P.; Valeri, S.; Benia, H. M.; Nilius, N.; Renaud, G. *Phys. Rev. B* **2008**, *78*, 195411.
(20) Ricci, D.; Bongiorno, A.; Pacchioni, G.; Landman, U. *Phys. Rev. Lett.* **2006**, *97*, 036106.
(21) Benia, H. M.; Lin, X.; Gao, H- J.; Nilius, N.; Freund, H.-J. *J. Phys. Chem. C* **2007**, *111*, 10528–10533.
(22) Yang, B.; Lin, X.; Gao, H- J.; Nilius, N.; Freund, H.-J. *J. Phys. Chem. C*, DOI 10.1021/jp100757y.
(23) Nieminen, J. A.; Niemi, E.; Rieder, K.-H. *Surf. Sci.* **2004**, *552*, L47–L52.
(24) Ho, W. *J. Chem. Phys.* **2002**, *117*, 11033–11061.
(25) Lauhon, L. J.; Ho, W. *Phys. Rev. B* **1999**, *60*, R8525–R8528. Nilius, N.; Wallis, T. M.; Ho, W. *J. Chem. Phys.* **2002**, *117*, 10947–10952.

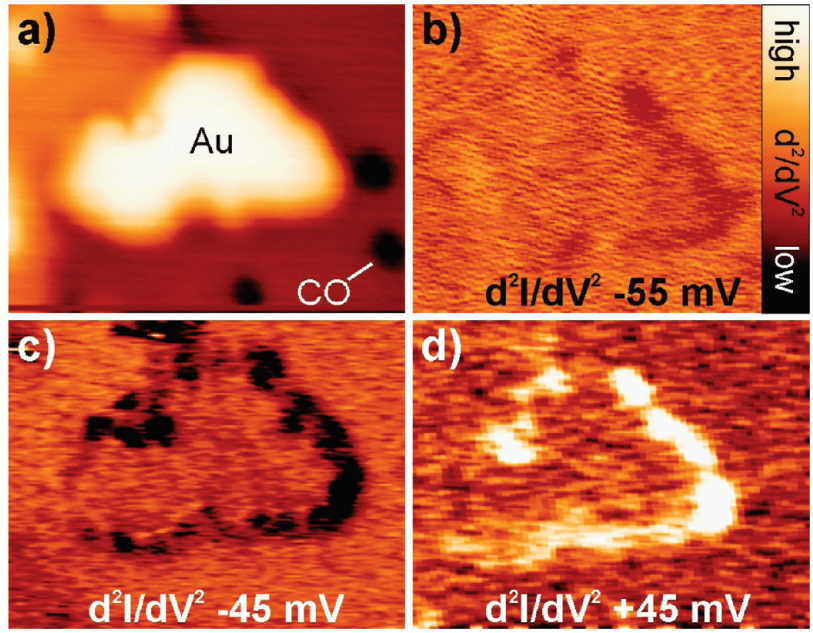

Figure 2. (a) STM topographic image and (b−d) corresponding second-derivative maps of a planar Au island saturated with CO (7.0×5.5 nm^2, 10pA). Due to the metallic tip state, the CO molecules are not resolved on the island but give rise to distinct energy-loss features at the island perimeter (c,d). The second-derivative contrast vanishes at bias voltages away from the CO vibrational modes (b).

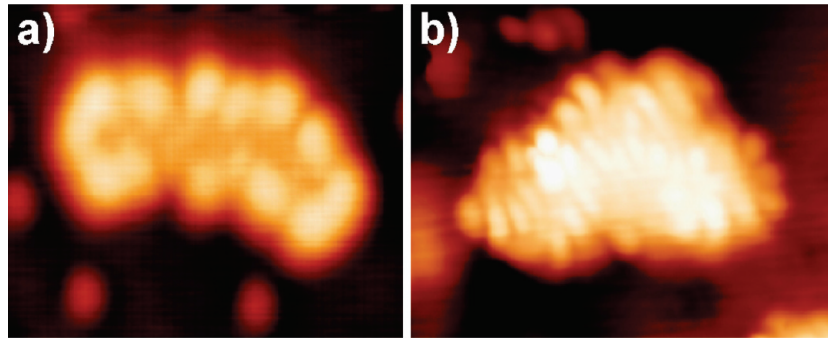

Figure 3. STM topographic images of (a) a bare and (b) a CO-saturated Au island on 2 ML MgO/Ag(001) (7.0×5.5 nm^2, 150 mV). Whereas the bare island is surrounded by a bright rim, indicating charge accumulation at the perimeter, the CO-covered island exhibits charge-density waves in the interior. The standing electron waves are due to electron displacement from the island boundary upon CO adsorption.

corroborates the CO attachment to edge and corner atoms of the Au islands.

The preferential CO binding to the island perimeter might be ascribed to two effects. On the one hand, the boundary atoms have a lower coordination than the ones enclosed in the Au plane. The same mechanism controls the CO adsorption on stepped metal surfaces.[26] On the other hand, the transfer electrons from the MgO/Ag support localize at the island perimeter, as the Coulomb repulsion between the extra charges becomes minimal in this configuration.[13] The charge localization can be inferred from the bright brim that emerges around adsorbate-free Au islands in STM images taken near E_F (Figure 3a). The brim reflects the availability of additional electronic states at the boundary, being introduced to accommodate the extra electrons from the support. According to DFT calculations,[9] the coordination effect clearly dominates the CO binding behavior. Whereas CO adsorbs with 0.72 eV to 3-fold coordinated edge atoms of a negatively charged Au_{12} island on MgO/Ag(001), it is nearly unbound to the 5-fold coordinated atoms in the interior. A similar binding enhancement is revealed for edge versus inner atoms of a neutral Au_{12} island on bulk MgO.[9] The extra electrons localized on the perimeter of charged islands counteract this trend, as they impede charge donation from the CO 5σ into the metal and hence increase the CO−Au repulsion.[17] The concomitant reduction of the CO binding strength is demonstrated with DFT. While CO binds with 0.81 eV to a neutral Au atom on bulk MgO, this value decreases to 0.21 eV for Au^- on the thin film.[10] Similarly, the CO binding energy at a corner of a Au_{12} reduces from 0.89 eV for the neutral to 0.72 eV for the negatively charged island.[9] Clearly, CO attaches to the island perimeter not because of but despite the extra charge, and the binding preference with respect to the top facet is governed by the reduced coordination of the edge atoms.

This conclusion is supported by the experimental observation that CO adsorption modifies the charge distribution within the Au islands. Prior to CO exposure, the transfer electrons from the MgO/Ag support are confined to the island perimeter, which gives rise to its bright appearance in the STM (Figure 3a). This specific contrast disappears after CO dosage, when standing

(26) Wang, H.; Tobin, R. G.; Lambert, D. K. *J. Chem. Phys.* **1994**, *101*, 4277–4287. Hammer, B. *Top. Catal.* **2006**, *37*, 3–16.

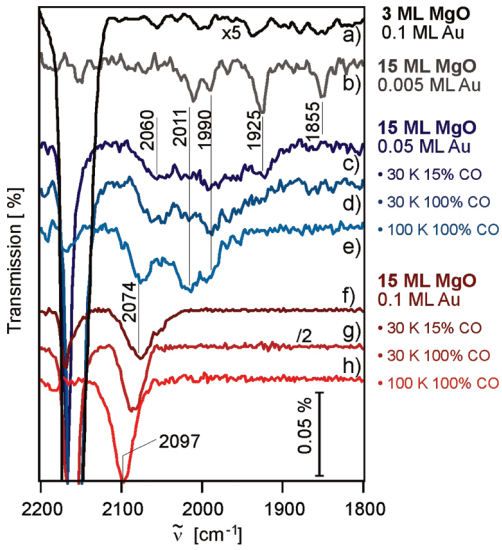

Figure 4. (a) Infrared absorption spectrum of CO adsorbed on a 3 ML MgO/Ag(001) film covered with 0.1 ML Au. (b−h) IR spectra taken on an electron-bombarded 15 ML thick MgO/Mo film covered with (b) 0.005 ML Au (CO saturation coverage, 100 K), (c) 0.05 ML Au (15% CO exposure, 30 K), (d) 0.05 ML Au (saturation coverage, 30 K), and (e) 0.05 ML Au (saturation coverage, 100 K). The spectra (f−h) were taken for 0.1 ML Au coverage and (f) 15 s CO exposure (30 K), (g) CO saturation coverage (30 K), and (h) after annealing the sample to 100 K.

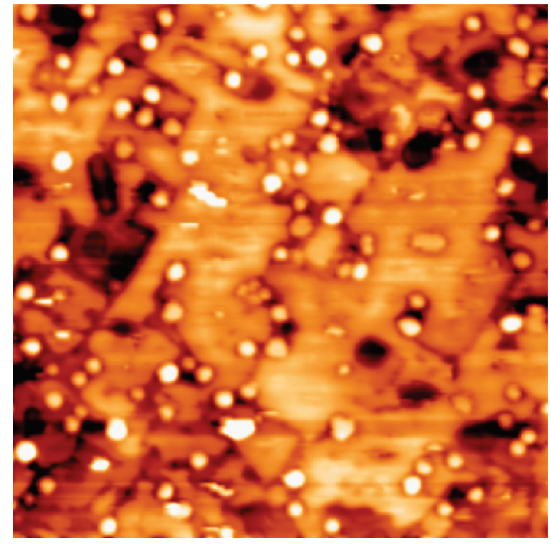

Figure 5. STM topographic image of Au clusters deposited on a 12 ML thick, electron-bombarded MgO/Mo(001) film (100 × 100 nm^2, 5.5 V, 20 pA). The aggregates preferentially nucleate at the dislocation lines in the film.

electron waves emerge in the island center (Figure 3b).[27] Apparently, the CO removes the localized charges from the perimeter sites by pushing them into the interior of the island. Also this finding is in line with DFT results for charged Au_{12} clusters on MgO/Ag(001).[9] A corner atom reduces its charge state from $-0.21|e|$ to $+0.16|e|$ upon CO attachment to minimize the Pauli repulsion with the CO 5σ orbital. The required energy for the charge delocalizing lowers the CO binding strength on a charged island by ∼25% compared to a neutral one.

The CO interaction with negatively charged island edges should also affect the vibrational properties of the molecule. A higher electron density in the Au promotes charge donation into the antibonding CO 2π* orbital, which weakens the internal CO bond and downshifts the CO stretching frequency.[17] Unfortunately, this expectation could not be proven with STM-IETS, as d^2I/dV^2 mapping at the CO stretch frequency (∼255 meV) results in an immediate CO desorption from the surface. We have therefore addressed this question with IR spectroscopy, being the method of choice to probe vibrational excitations. However, also these experiments did not produce convincing evidence for charge-mediated CO binding (Figure 4a, top spectrum). The respective IR spectrum taken for 0.1 ML Au dosed on 3 ML MgO/Ag(001) exhibits only a band at 2150 cm^{-1} that is assigned to CO on the MgO film but no conclusive signal from Au-bound molecules. The likely reason for the absence of Au−CO bands is the strong inclination of CO on the planar Au islands with respect to the surface normal, which impedes dipolar excitations due to the metal-surface selection rules of IRAS.[9] Furthermore, Au islands on the MgO film are characterized by a broad size and charge distribution, which gives rise to a spread of the CO stretching frequencies over an appreciable spectral range.[8] Due to this dispersion, the amplitude of individual absorption lines may drop below the detection limit and produce a rather featureless spectral background.

CO on Au Particles on Thick MgO/Mo Films. To demonstrate charging effects on the CO vibrational characteristic, we took an alternative approach to produce electron-rich Au clusters, namely Au exposure to thick, electron-bombarded MgO films on Mo(001). On thick insulating films, STM cannot be used to identify single CO molecules, as the required stabilization bias of more than +5 V is clearly incompatible with molecular imaging. The CO binding properties on such surfaces are however accessible to IRAS, whereas STM still provides information on the nucleation density and size of the Au aggregates. Figure 5 displays an STM topographic image of a 12 ML thick MgO/Mo film, being exposed to electrons to produce F^0 and F^+ centers. Those point defects that mainly form along step edges and misfit-induced dislocation lines are the preferential Au nucleation sites on the oxide film.[21] After dosing 0.05 ML Au at room temperature, Au particles develop on the surface that are one to two layers high and contain 30−50 atoms (Figure 5).

For the IRAS experiments shown in Figure 4, Au deposition was carried out at 30 K sample temperature, which increases the nucleation density and decreases the mean particle size. For the given coverage range of 0.1 to 0.005 ML Au, the size of Au deposits is expected to vary between a few tens of atoms down to monomers and dimers. The IRAS data in Figure 4b−h show bands ranging from 2090 cm^{-1} all the way down to 1990 cm^{-1} as well as a two isolated lines at 1925 and 1855 cm^{-1}. All bands are red-shifted compared to CO adsorbed on Au clusters on pristine MgO films, which are found between 2125 and 2100 cm^{-1} depending on the preparation conditions. The low-frequency lines that only occur at the smallest metal exposure (Figure 4b, gray line) are assigned to Au atoms adsorbed to regular terrace sites (1855 cm^{-1}) and F^0-centers (1925 cm^{-1}) on the basis of results in the literature.[12] All other bands can be explained by CO bound to negatively charged Au aggregates located on top of electron-rich surface defects.[8] In particular, the noisy features at ∼1990 and ∼2011 cm^{-1} are suggested to originate from CO adsorption to ultrasmall Au aggregates, e.g. dimers and trimers.

This assignment is corroborated by IR spectra taken at higher Au exposure (Figure 4c−e, blue lines). In addition to the low-

(27) Hövel, H.; Barke, I. *New J. Phys.* **2003**, *5*, 31.1.

frequency bands discussed before, new blue-shifted lines emerge in the frequency range around 2060 cm^{-1} that shift to 2070 cm^{-1} upon annealing to 100 K. For the highest coverage of 0.1 ML (Figure 4f−h, red lines), the spectra is dominated by a band at 2074 cm^{-1} while the strongly red-shifted bands disappear. Annealing the system to 100 K induces again a blue shift of the line to 2097 cm^{-1}. Inspection of the two data sets shown in Figure 4c−e and 4f−h reveals that neither the intensity nor the line shape of the Au-related bands changes when the CO coverage is increased from 15% to 100% of the saturation value. Annealing the systems to 100 K, on the other hand, leads to a blue shift of the lines that reaches 15 cm^{-1} for the bands at 2060 (Figure 4e) and 2080 cm^{-1} (Figure 4h). At 100 K, CO desorbs from the MgO film as evident from the reduction of the MgO-related CO-stretch bands between 2150 and 2180 cm^{-1}.[28] Together with the fact that the IR intensity of the Au-related bands is virtually unchanged, one may conclude that the shift of the resonance position upon annealing is caused by the vanishing vibrational coupling between the Au-bonded CO and molecules on adjacent MgO patches. The visibility of such shifts reflects the small size of the Au aggregates, as similar effects would be suppressed for large particles.

In general, the CO stretching frequencies experience a decreasing red shift with higher Au exposure and increasing cluster size, a phenomenon that can be rationalized in the following way. Assuming that each Au aggregate nucleates on a single color center and takes up one electron, the density of excess charges decreases in the larger particles, which reduces the amount of π-back-donation into the CO and hence the red shift of the stretch mode. A similar conclusion was drawn from CO adsorption experiments on charged gas-phase clusters, where the CO stretch mode was found to increase when going from Au_8^- (2050 cm^{-1}) to Au_8^+ clusters (2150 cm^{-1}).[14] This simple picture needs however to be modified in view of the earlier discussion. CO binds to the low-coordinated sites of the charged Au aggregates, which accommodate the extra electrons as well. The amount of π-back-donation now depends on the ability of the cluster to distribute the charge away from the CO adsorption site to lower the Pauli repulsion with the CO. Naturally, this ability diminishes with decreasing particle size, causing the charge transfer into the CO $2\pi^*$ to increase.

Based on these considerations, the experimental IR bands may be assigned. The bands above 2060 cm^{-1} that shift in an almost continuous fashion with Au exposure are produced by particles containing a few tens of atoms, whose charge density changes only gradually with size. The quasi discrete bands at 1990 and 2010 cm^{-1}, on the other hand, are characteristic for ultrasmall aggregates such as dimers. A direct assignment of these bands is difficult, as not only the size of the aggregate but also the nature of the oxide defect underneath determines the vibrational response. According to DFT calculations, Au dimers bound to F^0-centers interact only weakly with CO and produce a red shift of the stretching frequency of 194 cm^{-1}, whereas on F^+-centers the binding is sizable and the red shift is smaller (158 cm^{-1}).[9] However, also negatively charged Au_3^- and Au_4^- clusters produce a red shift of ~175 cm^{-1}. The experimental CO bands at 1990 and 2010 cm^{-1} are therefore compatible with several ultrasmall Au clusters, and no clear-cut assignment can be given.

Conclusions

Negatively charged Au particles on MgO thin films have been prepared by two different approaches and characterized with respect to their CO binding behavior. Whereas, on ultrathin films, the ad-particles charge up due to an electron transfer from the support, the charging on thicker films is realized by an electron donation from defects. In both cases, the excess electrons give rise to unusual CO adsorption properties, as deduced from STM and IRAS measurements. On planar Au islands on thin MgO films, the CO exclusively binds to the low-coordinated Au atoms along the island perimeter. The adsorption is accompanied by a redistribution of the cluster electrons away from the boundary toward the interior. On thicker films, the Au charging gives rise to an increasing red shift of the CO stretch mode with decreasing particle size, reflecting the gradual filling of the antibonding CO $2\pi^*$ orbital. Discrete steps in the frequency course hereby indicate the presence of Au aggregates with well-defined atom counts.

Our experiments provide insight into the role of excess charges on the adsorption behavior of spatially confined metal clusters on oxide supports. While studies using CO as a probe molecule are mainly of academic interest, other phenomena, e.g. the O_2 activation in oxidation reactions, strongly depend on the presence of charged ad-particles.[4] A detailed understanding of the interplay between charge state and adsorption behavior of metal particles is therefore crucial to optimize elementary processes in heterogeneous catalysis.

Acknowledgment. We are grateful to Gianfranco Pacchioni for many stimulating discussions. The work has been supported by the Humboldt Foundation (X.L.), the COST D41 network, the DFG through the "Cluster of Excellence UNICAT", and the Fonds der Chemischen Industrie.

JA101188X

(28) Sterrer, M.; Risse, T.; Freund, H.-J. *Surf. Sci.* **2005**, *596*, 222–228.